PHYSICAL REVIEW B
CONDENSED MATTER

THIRD SERIES, VOLUME 31, NUMBER 11 1 JUNE 1985

Sequential two-photon excitation processes of Nd^{3+} ions in solids

Gregory J. Quarles, George E. Venikouas,* and Richard C. Powell
Department of Physics, Oklahoma State University, Stillwater, Oklahoma 74078
(Received 7 November 1984)

The frequency-doubled and -tripled outputs of a high-power pulsed Nd-doped yttrium aluminum garnet laser were used to excite Nd^{3+} ions in hot crystals of $Y_3Al_5O_{12}$ and $Y_3Ga_5O_{12}$ and in a commercially available Nd-doped lithium silicate glass (ED-2). The fluorescence emission occurring as a result of two-photon excitation processes was studied for both of these excitation wavelengths. The variations of the intensities of the emission processes with laser pulse width show that the excitation processes are sequential stepwise absorption processes with real resonant intermediate states. A time-resolved spectroscopy technique developed previously was used to determine the excited-state absorption cross sections which are shown to be consistent with theoretically predicted values. The frequency-tripled laser excitation process terminates on a $5d$ level of Nd^{3+}, leading to a cross section over two orders of magnitude greater than that associated with the process occurring after frequency-doubled laser excitation which terminates on a level of the $4f$ configuration. Radiative and radiationless relaxation processes between $5d$ and $4f$ levels are also observed in these systems.

I. INTRODUCTION

High-power, picosecond-pulse lasers provide sources for studying spectroscopic properties of materials not easily observable under normal excitation conditions. Two important processes of this type are multiphoton absorption and intraconfigurational relaxation. Both of these processes are especially important in materials to be used in applications involving high levels of optical pumping. We recently reported initial results of studying the spectroscopic properties of $Y_3Al_5O_{12}$:Nd^{3+} [neodymium-doped yttrium aluminum garnet (Nd-YAG)] after excitation with high-power pulses of 30-picosecond duration.[1] The properties of two new metastable states were characterized, two different types of two-photon absorption processes were identified, and the $5d$-$4f$ radiationless relaxation rate was measured for this material. The work described here extends this investigation to provide a detailed understanding of these excitation and relaxation processes and to characterize their properties in different materials.

Using the time-resolved spectroscopy technique developed previously,[1] the two-photon absorption cross sections were measured for Nd-YAG for excitation wavelengths of 532.0 and 354.7 nm as a function of laser pulse width between 30 and 200 ps. For both cases, the results are shown to be consistent with sequential two-photon excitation processes (STEP). Similar results were observed on $Y_3Ga_5O_{12}$:Nd^{3+} neodymium-doped yttrium gallium garnet (Nd-YGaG) and on Nd-doped lithium silicate glass (ED-2), but not on other Nd-doped crystals. In addition, the $5d$-$4f$ radiationless relaxation rate in Nd-YGaG was measured to be similar to that found in Nd-YAG. In the glass host Nd^{3+}-Ce^{3+} energy transfer was observed.

II. EXPERIMENTAL PROCEDURE

Figure 1 shows a block diagram of the experimental setup. The Nd-YAG laser provides a pulse whose duration is controlled by changing the output coupler of the oscillator cavity and whose wavelength depends on the harmonic generation crystals used. The power of the excitation pulse incident on the sample is controlled by changing the laser power supply and by using neutral density filters. The sample fluorescence is analyzed by a $\frac{1}{4}$-m monochromator. For time-resolved spectroscopy measurements, an EG&G—Princeton Applied Research (EGG—PAR) gated optical multichannel analyzer with a silicon diode array is used for detection. For lifetime measurements, an EGG—PAR boxcar integrator/signal averager combination is used with an RCA C31034 photomultiplier tube for detection. A beam splitter picks off part of the pulse to monitor the shot-to-shot intensity variations of the laser.

Three samples were investigated in this work: YAG:Nd^{3+} (1.18×10^{20} cm^{-3}); YGaG:Nd^{3+} (3.24×10^{19}

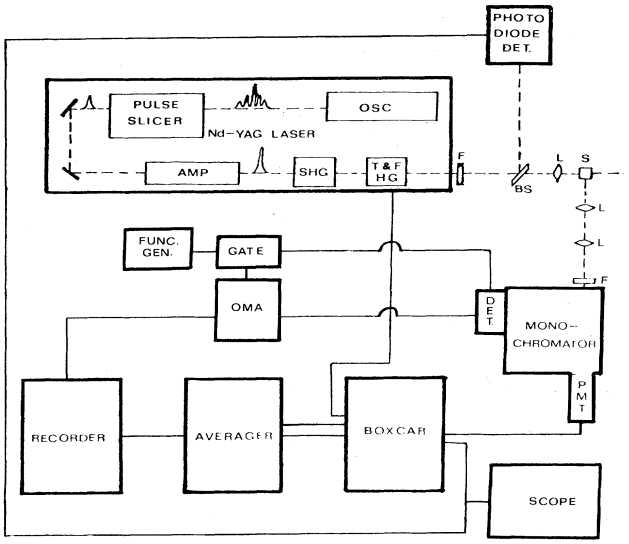

FIG. 1. Block diagram of experimental apparatus. The laser is a passively mode-locked Nd-YAG system with a single-stage amplifier and frequency-doubling, -tripling, and -quadrupling crystals. *F*, filter; BS, beam splitter; *L*, lens; and *S*, sample. Time-resolved fluorescence spectra are recorded using a silicon diode array detector and a gated optical multichannel analyzer (OMA). Fluorescence lifetimes are measured using a photomultiplier tube detector and a boxcar integrator/signal averager combination.

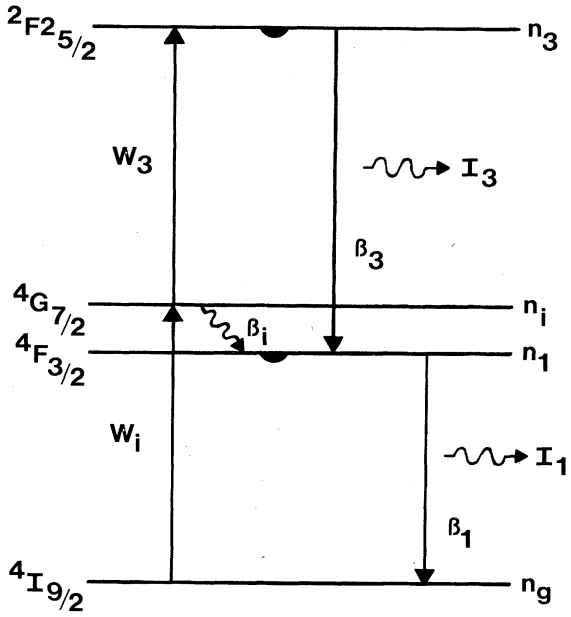

FIG. 2. Rate diagram for interpreting the spectral dynamics observed after high-power excitation at 532.0 nm. The W's represent excitation rates and the β's represent decay rates. The n's are the populations of the various energy levels and the I's are the fluorescence emission intensities.

cm^{-3}); and ED-2:Nd^{3+} (1.83×10^{20} cm^{-3}). The composition of the glass host in mole percent is $60SiO_2$, $27.5Li_2O$, 10CaO, and $2.5Al_2O_3$ with $0.16CeO_2$ and $0.35Nd_2O_3$. Some of the general spectroscopic properties of these samples have been reported previously.[2–5]

III. RESULTS FOR 532.0 nm PUMPING

The frequency doubled output of the Nd-YAG laser was used to excite the samples at 532.0 nm. It was shown in Ref. 1 that this wavelength results in two-photon excitation of the $^2(F2)_{5/2}$ level which is the highest energy metastable state of the $4f^3$ electronic configuration of the Nd^{3+} ion. The properties of the fluorescence emission from this level are summarized in Ref. 1. A simplified rate diagram for describing the pumping and decay dynamics under this excitation condition is shown in Fig. 2. One of the Stark components of the $^4G_{7/2}$ level acts as a real intermediate state for the two-photon transitions. The ions excited to this intermediate state either relax radiationlessly to the $^4F_{3/2}$ metastable state or are re-excited to the $^2(F2)_{5/2}$ state. The W_k and β_k parameters represent the appropriate pumping and decay rates. The fluorescence emission can be monitored from level 3 after two-photon excitation and from level 1 after one-photon excitation. The rate equations describing the time evolution of these fluorescence emissions have been solved previously.[1]

Figure 3 shows the ratios of the measured integrated fluorescence intensities of the transitions from level 3 and level 1 for Nd-YAG using different excitation pulse widths. These intensities have been corrected for quantum efficiencies, branching ratios, and the spectral sensitivity of the equipment. The observed exponential variation of the intensity ratio with time after the excitation pulse is consistent with the results reported previously.[1] The important new information shown in Fig. 3 is that the slope and intercept of this time evolution changes with the pulse width of the laser excitation. This type of varia-

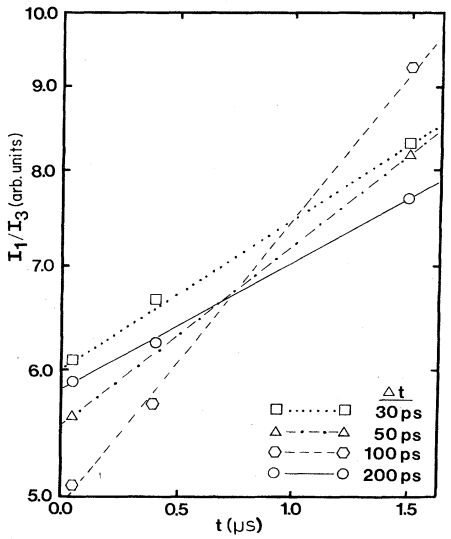

FIG. 3. Time evolution of the ratios of the integrated fluorescence intensities of the emission from the $^4F_{3/2}$ and $^2(F2)_{5/2}$ metastable states after 532.0 nm excitation of different pulse widths for Nd-YAG.

tion will occur for two-photon transitions involving real resonant intermediate states but not for transitions involving virtual intermediate states. Therefore these results show that a sequential two-photon excitation process is responsible for the fluorescence from the $^2(F2)_{5/2}$ level.

The values of the fluorescence intensities immediately after the excitation pulse can be used to determine the excited-state absorption cross section for the STEP mechanism,

$$\sigma_{i3}=[\beta_1'/\beta_3'][I_3(0)/I_1(0)][(h\nu_1)/(h\nu_3)][(\beta_i\,\Delta t)/(0.375I_p)]\ , \tag{1}$$

where again the corrected values for $I_k(0)$ are implied. The β_k' represent the radiative decay rates, Δt is the laser pulse width, and I_p is the photon flux per pulse. A major simplification which has been made in deriving the expression in Eq. (1) is using $P(t)=(0.375/\Delta t)$ for the pulse-time dependence instead of the full Gaussian expression

$$P(t)=(0.375/\Delta t)\exp\{-2.77[(t-t_0)/\Delta t]^2\}\ . \tag{2}$$

In order to evaluate the excited-state absorption cross section using Eq. (1), it is necessary to estimate a value for the decay rate of the intermediate state of the STEP transition. This can be done by considering the spectral line shape of the absorption transition from the ground state to the $^4G_{7/2}$ level. The absorption spectra in this region are shown in Fig. 4 for the three samples. The structure and asymmetry of these absorption lines are due to unresolved Stark components. An estimate of the full width at half maximum of an individual Stark component can be obtained by deconvoluting these spectral shapes. At room temperature, these linewidths should be dominated by lifetime broadening processes. Therefore the measured width of a level can be used to determine the decay rate from the level. This analysis gives a value of $\beta_i=8.4\times10^{12}$ Hz for the YAG:Nd sample. Using this value along with the measured values of the fluorescence intensities and the excitation pulse intensity, and the radiative decay rates of the metastable states determined previously,[1] Eq. (1) gives the values of the excited-state cross section for the STEP transition.

Figure 5 shows the variation of σ_{i3} with excitation pulse width for the Nd-YAG sample. The results show a direct correspondence between σ_{i3} and Δt as predicted by Eq. (1). However the best fit to the data is a line with a slope slightly greater than the predicted value of one. This is probably associated with the simplification used in describing the pulse shape in Eq. (1).

Table I lists the values of the parameters obtained in this study. Experimental error in determining the corrected values of the intensities limits the accuracy of the σ_{i3} value to $\pm1\times10^{-19}$ cm^2. A similar analysis was made of the same STEP mechanism in Nd-YGaG and in Nd-ED-2. The values of β_i and σ_{i3} for Nd-YGaG are similar to those found for Nd-YAG. The extensive inhomogeneous line broadening in the glass host makes it impossible to use the spectrum shown in Fig. 4 to obtain a value for β_i for Nd-ED-2 and therefore the value of σ_{i3} cannot be determined by this method.

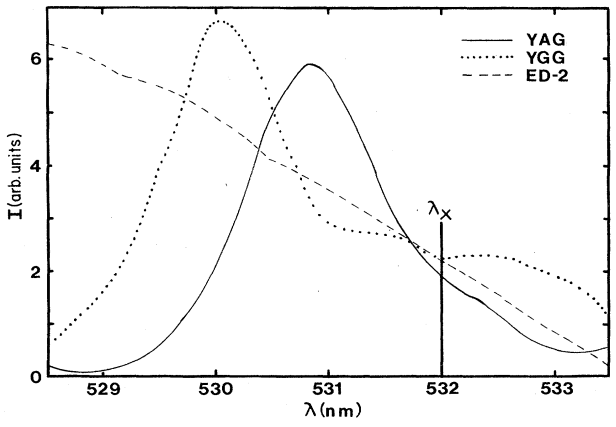

FIG. 4. Absorption spectra of Nd^{3+} in three hosts in the region of 532.0 nm excitation.

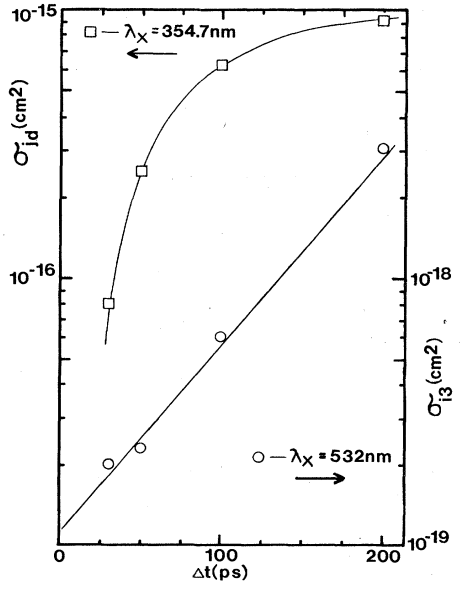

FIG. 5. Variation of the excited state absorption cross sections σ_{i3} (532.0 nm excitation) and σ_{id} (354.7 nm excitation) with excitation pulse width for Nd-YAG.

TABLE I. Summary of parameters ($\Delta t = 30$ ps; $T = 300$ K).

Parameter	Host YAG	YGG	ED-2
τ_1 (μs)	220	264	320
τ_2 (μs)	0.3	0.3	0.4
τ_3 (μs)	3.0	2.0	1.0
τ_d (ns)	2.0	4.8	
β_i (Hz)	8.4×10^{12}	9.0×10^{12}	
β_j (Hz)	2.7×10^{13}	4.0×10^{13}	
σ_{i3} (cm^2)	2.1×10^{-19}	3.5×10^{-19}	
σ_{jd} (cm^2)	8.2×10^{-17}	6.5×10^{-17}	

IV. RESULTS FOR 354.7 nm EXCITATION

The spectral dynamics are more complex after excitation by the frequency-tripled output of the Nd-YAG laser.[1] Figure 6 shows a simplified rate equation diagram to describe the results. The tripled output of the Nd-YAG laser is in resonance with a transition from the ground state to one of the Strak components of the $^4D_{3/2}$ level. Electrons excited to this level can either relax radiationlessly to the $^2P_{3/2}$ metastable state or undergo a second photon absorption process to one of the $5d$ levels. The properties of the $^2P_{3/2}$ metastable state for Nd-YAG were characterized in Ref. 1. The electrons excited to the $5d$ level relax back to the $^2(F2)_{5/2}$ metastable state and decay radiatively as described in the preceding section.

The various excitation and decay rates and the level populations are designated in Fig. 6. The rate equations for this model were solved in Ref. 1 and the results predict the time evolution of the ratio of the fluorescence intensities from level 2 to level 3 to decrease exponentially. Figure 7 shows the time dependence of I_2/I_3 for four different excitation pulse widths. An exponential decrease is seen for each case as predicted.

The fact that the slopes and intercepts of the curves in Fig. 7 are different for different pulse widths again shows that the two-photon excitation mechanism involves a resonant, real intermediate state. The cross section for the excited-state absorption part of this STEP mechanism is given by Eq. (1) with the subscripts designating levels 1 and i being replaced by 2 and j. The procedure described in the preceding section for estimating the relaxation rate of the intermediate level can be applied to find values for β_j using the absorption spectra in the region of the $^4D_{3/2}$ level shown in Fig. 8. The values obtained from this procedure are listed in Table I and σ_{jd} is plotted versus Δt for the Nd-YAG sample in Fig. 5. Experimental error in determining the corrected values of the intensities limits the accuracy of the σ_{jd} value to $\pm 8\times10^{-18}$ cm^2.

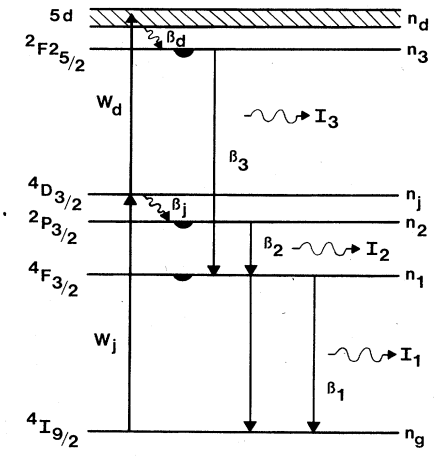

FIG. 6. Rate diagram for interpreting the spectral dynamics observed after high-power excitation at 354.7 nm. The W's represent excitation rates and the β's represent decay rates. The n's are the populations of the various energy levels and the I's are the fluorescence emission intensities.

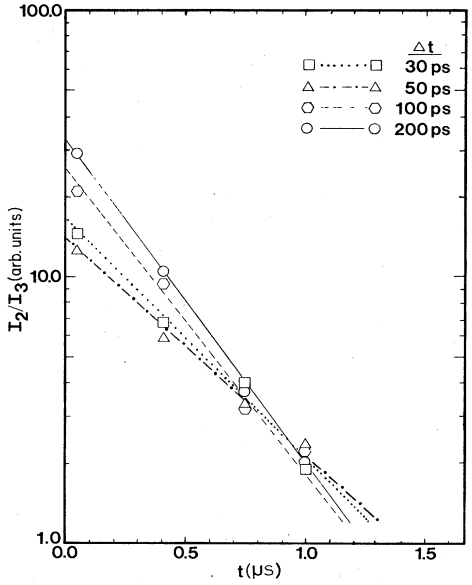

FIG. 7. Time evolution of the ratios of the integrated fluorescence intensities of the emission from the $^2P_{3/2}$ and $^2(F2)_{5/2}$ metastable states after 354.7 nm excitation of different pulse widths for Nd-YAG.

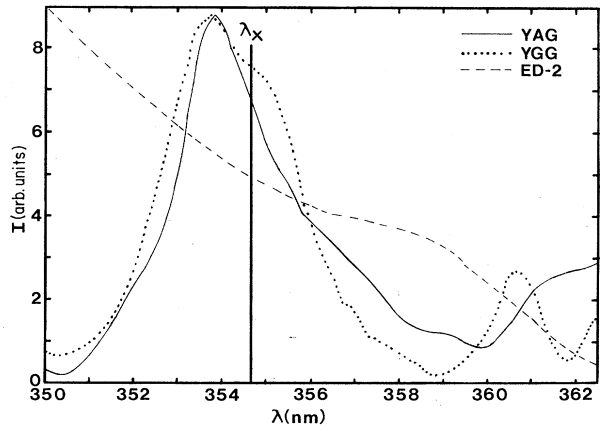

FIG. 8. Absorption spectra of Nd^{3+} in three hosts in the region of 354.7 nm excitation.

Similar measurements were made on the Nd-YGaG and Nd-ED-2 samples and the results are given in Table I. The magnitudes of both the σ_{jd} and the β_j parameters are similar for the two crystalline samples. However it was not possible to determine accurate values for these parameters for the glass sample due to the spectral characteristics shown in Figs. 8 and 9. The extremely broad, unresolved shape of the $^4D_{3/2}$ absorption band prevents accurate evaluation of β_j. Figure 9 compares the fluorescence emission of Nd-ED-2 in the 400 nm spectral region after 532.0 nm STEP excitation and after 354.7 nm STEP excitation. The former process leads to line emission from the $^2(F2)_{5/2}$ metastable state with a fluorescence decay time of 1.06 μs whereas the latter type of excitation results in broad band fluorescence with a 40 ns lifetime. The broad band is attributed to radiative emission from the $5d$ level of the Ce^{3+} ions present in the host glass excited by energy transfer from the Nd^{3+} ions.

The variation of σ_{jd} with excitation pulse width shown in Fig. 5 for Nd-YAG is generally in agreement with the prediction of Eq. (1). However, there appears to be an additional time dependence which causes the cross section to decrease more rapidly at smaller values for the excitation pulse width. This can be attributed to the finite value of β_d which has been ignored in the derivation of the simplified expression for σ_{jd} given in Eq. (1). The fluorescence emission from the $^2(F2)_{5/2}$ level exhibits an initial rise after 354.7 nm STEP excitation through the $5d$ level which is not observed after 532.0 nm STEP excitation or direct excitation of this metastable state. The time at which the fluorescence reaches its maximum value, t_m, can be related to the decay rates of the $5d$ and the $^2(F2)_{5/2}$ levels through the expression[6]

$$t_m = \tau_3 \tau_d \ln(\tau_d/\tau_3)/(\tau_d - \tau_3) \ . \quad (3)$$

The values determined for the relaxation time of the $5d$ level for the two crystalline samples are of the order of a few nanoseconds as listed in Table I. This d-f relaxation time can affect the value for $I_3(0)$ used in Eq. (1) to determine the magnitude of σ_{jd}.

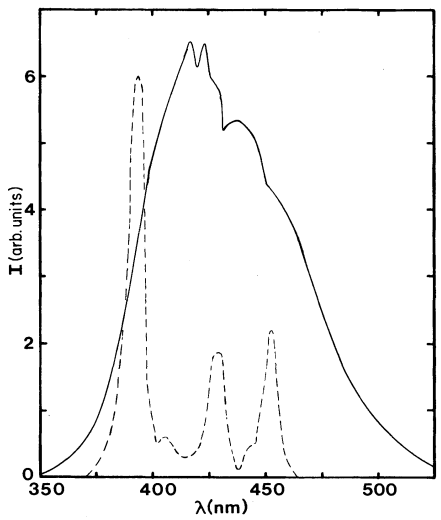

FIG. 9. Fluorescence spectra of Nd-ED-2 near 400 nm after high-power excitation at 532.0 nm (dashed line) and at 354.7 nm (solid line).

V. DISCUSSION AND CONCLUSIONS

The results obtained in this study show that the spectroscopic properties of Nd^{3+} ions in YGaG and ED-2 hosts under high-power, picosecond-pulse excitation are similar to those observed in YAG.[1] The fluorescence lifetimes of the three metastable states of the $4f^3$ configuration observed in this investigation are listed in Table I. The nonradiative decay rate for the $5d$-$4f$ process in Nd-YGaG is similar to that found for Nd-YAG. However, in the ED-2 glass host Nd^{3+} multiphonon excitation with 354.7 nm pumping resulted in energy transfer to Ce^{3+} which decayed radiatively. The measured fluorescence decay time is similar to the $5d$ lifetime found previously by directly pumping Ce^{3+} in ED-2 (Refs. 7 and 8) and that measured for Ce^{3+} ions in YAG.[9] The band position shown in Fig. 9 appears to be shifted to longer wavelengths compared to the Ce^{3+} emission shown in Ref. 7. This can be attributed to the effects of reabsorption. The overlap of the fluorescence with the Ce^{3+} and Nd^{3+} absorption bands on the high-energy side of the emission cuts off the band in this region. The undistorted band shape can be observed only for very small samples with very small Ce^{3+} concentrations and observation of the fluorescence from the front face. To prove that the observed emission is associated with Ce^{3+}, we studied two other glass samples under the same excitation conditions. One contained Ce^{3+} only and the other contained only Nd^{3+}. The first exhibited the same broad band shown in Fig. 9 and the other showed the series of sharper lines.

Similar experiments performed on NdP_5O_{14} and YVO_4:Nd crystals with 532.0 nm excitation gave significantly different results from those reported above. In the former crystal no STEP mechanism was observed even with high excitation powers. In the latter crystal the STEP mechanism resulted in the fluorescence of the host vanadate emission band indicating delocalization of the excited electron. These different types of responses appear to be associated with the location of the $^2(F2)_{5/2}$ energy level with respect to the host band edge. This will be the subject of future investigations.

There have been several other investigations of multiphoton excitation processes of Nd^{3+} ions in solids.[10–13] However, these have each involved experimental conditions very different from the high-power picosecond-pulse excitation used here. Under some conditions, two-photon processes involving virtual intermediate states have been observed.[10] We were unable to observe such processes using the fundamental emission from the Nd-YAG laser with 30 ps pulses. Results of other studies have been interpreted using theoretical models involving virtual intermediate states even though resonant enhancement due to real intermediate states was present.[11,12] A model involving a STEP mechanism was employed in Ref. 13, but no unambiguous evidence was provided to justify this interpretation.

The time-resolved spectroscopy technique used here provides a sensitive experimental method for obtaining

two-photon absorption cross sections for the crystalline materials investigated here. However, the problem of inhomogeneous broadening in the glass sample demonstrates the limitation of this technique. The more conventional pulse-probe technique is required to obtain the transition cross section in this case. The data obtained from these measurements can be interpreted either in terms of two-photon processes involving virtual intermediate states or the STEP mechanism. In Ref. 1 we arbitrarily chose to use the former approach since it is more general and no evidence supporting either type of mechanism was available. However, the variation of the two-photon excitation efficiency with excitation pulse width reported here conclusively demonstrates that STEP mechanisms are responsible for both types of two-photon transitions which were investigated. The cross sections for the first steps in these two sequential processes have been tabulated previously for Nd-YAG.[14] Cross sections for $4f$-$4f$ transitions of Nd^{3+} in glass hosts are known to be smaller by about an order of magnitude due to inhomogeneous broadening.[15] The magnitudes of the cross sections measured for the second steps in the two-photon processes excited by 532.0 nm pulses are similar to those of the first steps. Theoretical estimates for these cross sections can be obtained from the expression

$$\sigma_{kl}=(\beta^r_{lk}\lambda^2_{kl})/(8\pi c n_0^2\,\Delta\nu_{kl})\ . \tag{4}$$

This can be applied to the data obtained on Nd-YAG using the branching ratios for the $^2(F2)_{5/2}$ level[1] and treating the transition linewidth as the convolution of the widths of the intermediate and final levels. The theoretically predicted cross section is 4.5×10^{-19} cm^2 which is in good agreement with the measured values.

The magnitudes of the cross sections of the second steps of the two-photon transitions after 354.7 nm excitation are significantly greater than those measured for the STEP mechanism involving 532.0 nm excitation. This is because the $4f$-$5d$ transition involves states of different parity and therefore is an allowed transition. Equation (4) cannot be applied to the Nd-YAG data for this case since it uses the fluorescence lifetime of the final state of the absorption transition and the $5d$ level does not exhibit radiative emission for this material.

In conclusion, the results reported here provide evidence for two types of STEP mechanisms in Nd-doped materials and supply new information about $5d$ radiationless relaxation transitions. Enhancing our understanding of these processes can be important in determining the spectral dynamics of these laser materials under high-power, fast pulse excitation conditions. This may be relevant to developing uv or cascade laser pumping schemes.

ACKNOWLEDGMENTS

This work was sponsored by the U.S. Army Research Office and by the National Science Foundation under Grant No. DMR-82-16551. The glass samples were provided by Lawrence Livermore National Laboratory and the authors benefited by helpful discussions with M. J. Weber, W. F. Krupke, S. E. Stokowski, and M. D. Shinn.

*Present address: Electronics Division, Union Carbide Corporation, P.O. Box 6381, Washougal, WA 98671.

[1]G. E. Venikouas, G. J. Quarles, J. P. King, and R. C. Powell, Phys. Rev. B **30**, 2401 (1984).
[2]L. D. Merkle and R. C. Powell, Phys. Rev. B **20**, 75 (1979).
[3]M. Zokai, R. C. Powell, G. F. Imbusch, and B. DiBartolo, J. Appl. Phys. **50**, 5930 (1979).
[4]R. C. Powell, D. P. Neikirk, and D. Sardar, J. Opt. Soc. Am. **70**, 486 (1980).
[5]L. D. Merkle, R. C. Powell, E. E. Freed, and M. J. Weber, J. Lumin. **24/25**, 755 (1981).
[6]B. DiBartolo, *Optical Interactions in Solids* (Wiley, New York, 1968).
[7]R. R. Jacobs, C. B. Layne, M J. Weber, and C. F. Rapp, J. Appl. Phys. **47**, 2020 (1976).
[8]S. E. Stokowski, 1979 Laser Program Annual Report, Lawrence Livermore National Laboratory Report No. UCRL-50021-79, 1979, p. 2—156 (unpublished).
[9]M. J. Weber, Solid State Commun. **12**, 741 (1973).
[10]S. Singh and J. E. Geusic, in *Optical Properties of Ions in Crystals*, edited by H. M. Crosswhite and H. W. Moos (Interscience, New York, 1967), p. 493.
[11]P. A. Apanasevich, R. I. Gintoft, V. S. Korolkov, A. G. Makhanek, and G. A. Skripko, Phys. Status Solidi B **58**, 745 (1973).
[12]M. A. Kramer and R. W. Boyd, Phys. Rev. B **23**, 986 (1981).
[13]B. R. Reddy and P. Venkateswarlu, J. Chem. Phys. **79**, 5845 (1983).
[14]W. F. Krupke, IEEE J. Quantum Electron. **QE-7**, 153 (1971).
[15]W. F. Krupke, IEEE J. Quantum Electron. **QE-10**, 450 (1974).